Table of Contents

Supplemental Table I: Androgen Therapies and Metastatic Sites of HRPC Cases*

A#	Gleason Score at Dx	Androgen-targeted therapies	Assayed Mets
2	7	leuprolide, Flutamide,	Liver
7	9	leuprolide,Flutamide,	Subdural
8	6	goserelin,Flutamide	Liver
9	7	leuprolide,Flutamide,	Periportal LN
10	8	goserelin,flutamide	Perigastric LN
16	7	leuprolide,flutamide	Adrenal
17	7	leuprolide,flutamide	Hilar LN
19**	8	leuprolide,flutamide	Pelvic LN
19**	8	leuprolide,flutamide	Bone (Humerus)
21	7	leuprolide,flutamide	Iliac crest soft tissue
23	7	goserelin	Liver
24	6	leuprolide,flutamide	Pericardial Met
26	8	goserelin,flutamide	Bone (T12)
27	7	leuprolide,flutamide	Axillary LN
28	7	leuprolide,flutamide, orchiectomy	Anterior Mediastinal LN
29	6	goserelin,flutamide	Inguinal LN
30	7	leuprolide,flutamide	Liver
31	6	goserelin,flutamide	Subdural
32	8	orchiectomy	Bone (Rib)
33	7	orchiectomy	Subdural
34	5	leuprolide,flutamide	Liver

*A total of 21 sectioned, pathologically and anatomically validated metastatic hormone refractory prostate cancer lesions derived from 20 autopsy cases were prepared and assayed.
**Two distant mets from case number 19 were assayed.

Supplemental Table II: Primer Sets Used in the Study and the Corresponding Amplicon Data

Primer Sets	Forward Primer	Reverse Primer	Amplified Transcript Size (bp)
P1 (Fig.1A)	TGTCACTATGGAGCTCTCACATGTGG	CACCTCTCAAATATGCTAGACGAATCTGT	AR-V1: 842 AR-V2: 959 AR-V3: 1126 AR-V4: 1243
P2 (Fig.1A)	TGTCACTATGGAGCTCTCACATGTGG	GTACTCATTCAAGTATCAGATATGCGGTATCAT	AR-V5: 888 AR-V6: 968
P3 (Fig.1A)	TGTCACTATGGAGCTCTCACATGTGG	CTGTGGATCAGCTACTACCTTCAGCTC	AR-V7: 834
P4 (Fig.1C)	GTTGCTCCCGCAAGTTTCCTTCTC	CTGTTGTGGATGAGCAGCTGAGAGTCT	AR-V1 full-length ORF: 2134
P5 (Fig.1C)	GTTGCTCCCGCAAGTTTCCTTCTC	TTTGAATGAGGCAAGTCAGCCTTTCT	AR-V7 full-length ORF: 2113
P6 (Fig.2A)	CCATCTTGTCGTCTTCGGAAATGTTATGAAGC	CTGTTGTGGATGAGCAGCTGAGAGTCT	AR-V1: 145
P7 (Fig.2A)	CCATCTTGTCGTCTTCGGAAATGTTATGAAGC	TTTGAATGAGGCAAGTCAGCCTTTCT	AR-V7: 125
P8 (Fig.2A)	CCATCTTGTCGTCTTCGGAAATGTTATGAAGC	AGCTTCTGGGTTGTCTCCTCAGTGG	AR protoype: 143
SF3A3 (Fig. 2A)	TACGAAAGGAGGAGCTCAATGCAA	AGATCTCATTTGGGTGCTTCCGGT	SF3A3: 107

Supplemental Table III. Summary of Transcribed Genomic Fragments Within Human AR Gene Introns.

Intron	Accession ID	Size(bp)	Identity	Start*	End**
1	AA886614	231	99.6%	66722674	66722904
1	AA577938	293	99.0%	66723711	66724004
1	AW973726	294	100.0%	66723711	66724004
1	R89771	382	100.0%	66725430	66725814
1	AI827337	490	100.0%	66750976	66751465
1	AW028775	437	99.8%	66772546	66772983
2	BF327858	202	99.6%	66791497	66791698
2	BE007634	450	99.6%	66791497	66791950
2	BE006793	355	100.0%	66819126	66819482
3	CV379421	270	100.0%	66826610	66826880
3	CN283227	674	99.3%	66829412	66830085
3	BF846156	538	99.7%	66831722	66832259
4	None				
5	None				
6	None				
7	None				

* Starting position coordinates on human chromosome X according to Reference Human Genome Assembly (March 2006 release, HG18)
**Ending position coordinates on human chromosome X according to Reference Human Genome Assembly (March 2006 release, HG18)

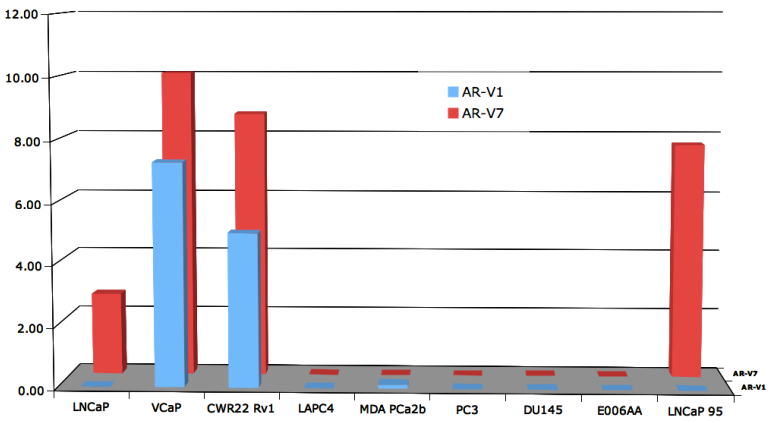

Supplemental Figure 1. Real time RT-PCR analysis of AR variants V1, and V7 in human prostate cancer cell lines. Normalized expression values (in $\log_2$ scale) for AR-V1 (blue) and AR-V7 (red) derived from comparative threshold analysis were shown in 9 human prostate cancer cells lines. LNCaP95 is an androgen-independent cell line derived from long-term continuous culture of LNCaP cells in androgen-depleted conditions, provided by Dr. Alan K. Meeker (Johns Hopkins University, Baltimore, MD). VCaP and E006AA prostate cancer cells were provided by Dr. John T. Isaacs (Johns Hopkins University, Baltimore, MD). Other human prostate cancer cells lines were obtained from the American Type Culture Collection (Rockville, MD).

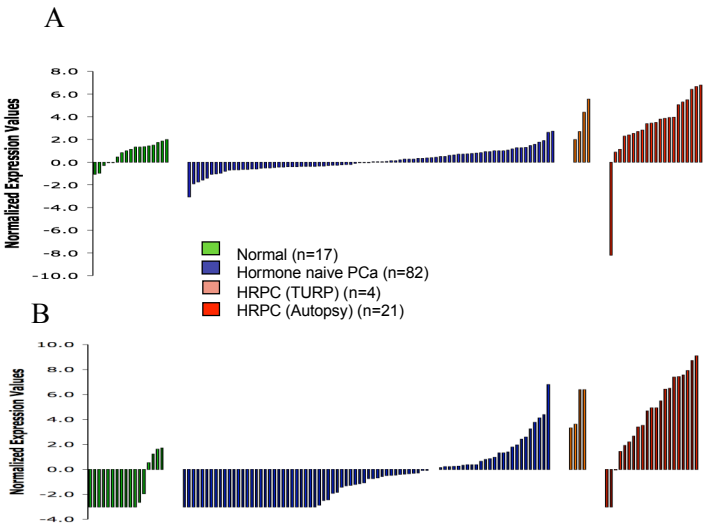

Supplemental Figure 2: Quantitative real-time RT-PCR results of prototype AR (A) and AR-V1 (B) in 124 clinical prostate specimens. Normalized expression values (in $\log_2$ scale) from comparative threshold analysis were centered with the median of measurable values in 82 RRP cases set at zero. Normal (n=17): normal prostate tissues from radical retropubic prostatectomy (RRP) specimens; Hormone Naïve PCa (n=82): PCa samples from RRP specimens; HRPC (TURP) (n=4): HRPC samples from transurethral resection of prostate (TURP); HRPC (autopsy) (n=21): metastatic HRPC samples from autopsies (Supplemental Table I).

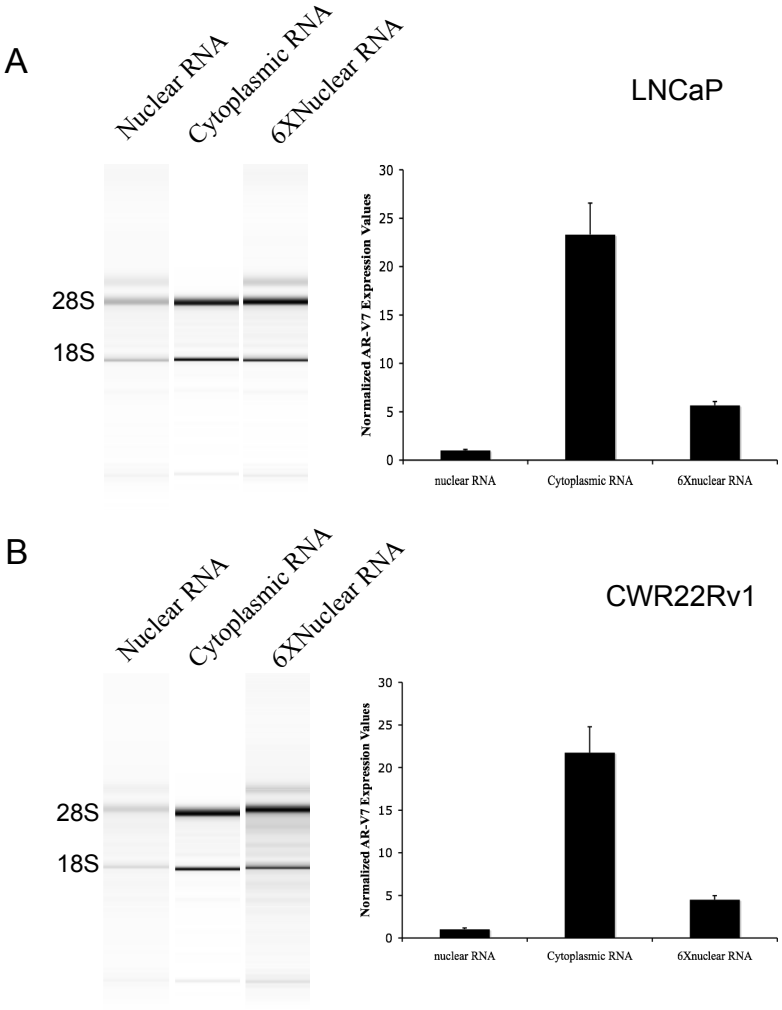

Supplemental Figure 3: Detection of AR-V7 transcripts using cytoplasmic or nuclear RNA extracted from LNCaP cells (A) and CWR22Rv1 cells (B). The Agilent Bioanalyzer electropherograms were shown to the left and the expression fold differences relative to the average value of nuclear RNA (from threshold cycle analysis) were shown to the right. The three samples for each cell line correspond to nuclear and cytoplasmic RNA isolated from equal number of cells , and nuclear RNA from 6 fold excess of cells (6Xnuclear RNA) to equalize the input nuclear RNA quantity with cytoplasmic RNA, as RNA yield/cell is ~6 fold higher in the cytoplasm than in then nucleus. Note that nuclear RNA is enriched for precursor rRNA (band above 28S rRNA). Also note that mature rRNA, but not mRNA, should be expected to be present in the nucleolus.

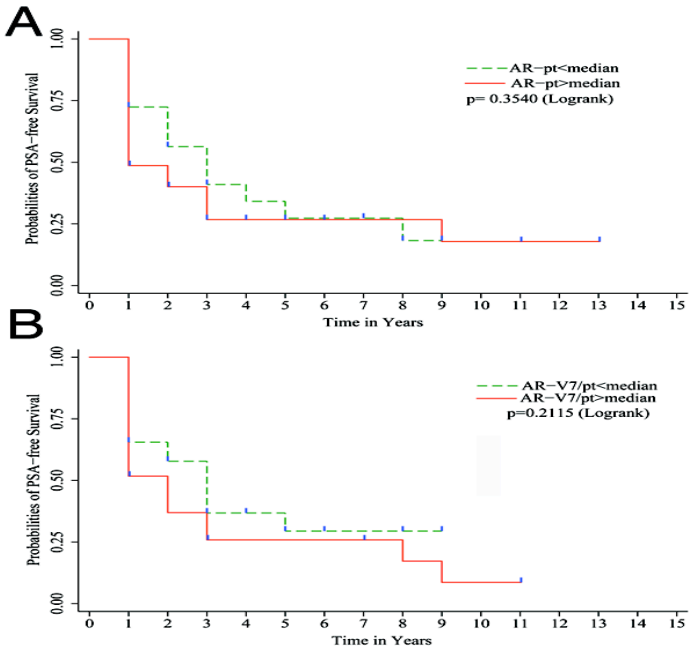

Supplemental Figure 4. Kaplan-Meier plot comparing progression free survival in 66 patients with lower than median and higher than median expression of prototype AR (AR-pt) expression (A) or ratio of AR-V7/AR-pt (B). The median value was identified based on all RRP cases (n=82) with measurable data points to be consistent with all similar analyses including data presented in Figure 2B. The survival curves were compared using the Log-rank test. And p values of the tests were provided. Follow-up years were marked on the X axis. Censored subjects were marked with vertical ticks in blue. Note that the PSA recurrence status was annotated in years, not months.

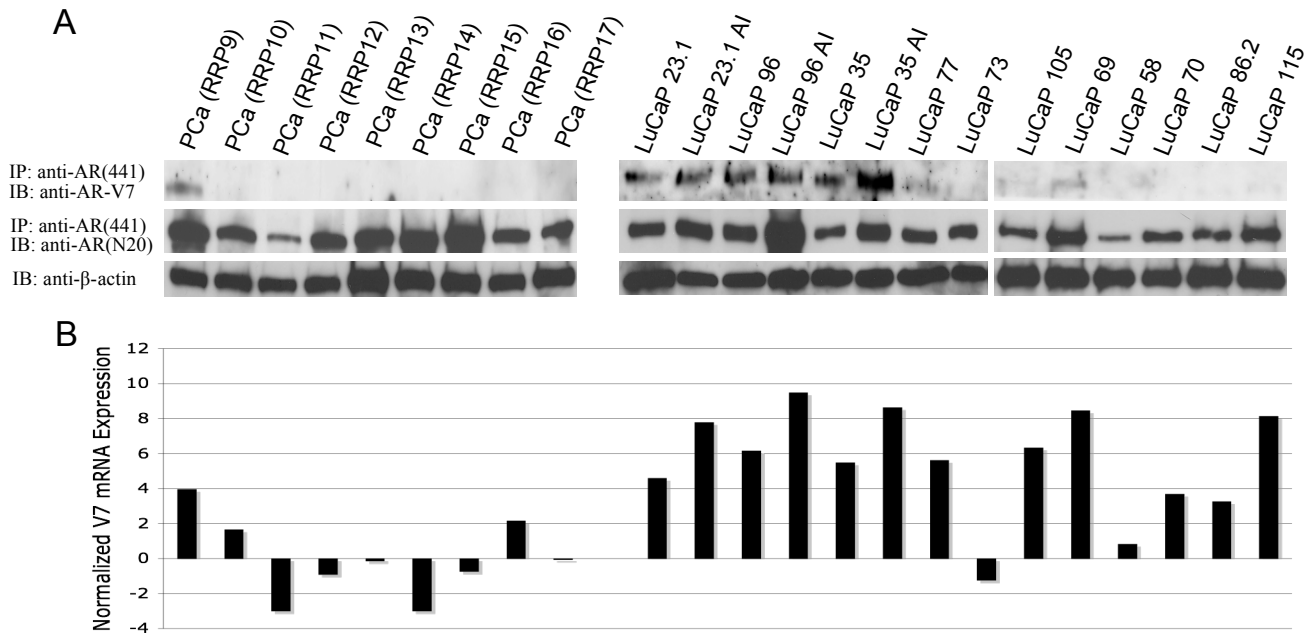

Supplemental Figure 5. Protein (A) and mRNA (B) expression analysis in 9 hormone naïve RRP cases and 14 LuCaP human prostate cancer xenografts. Detection of AR-V7 and prototype AR protein was carried out using standard western immunoblots (IB) following enrichment of AR proteins by immunoprecipitation (IP) using the anti-AR(441) antibody, while detection of the control β-actin protein was carried out using regular protein lysate matched in quantity to the input lysate for IP . Note that data from different protein blots were not cross-comparable as experimental variables were different while the mRNA data should be comparable across the all samples as AR-V7 mRNA expression levels were normalized (in $\log_2$ scale) and centralized to the median of the 82 RRP cases as presented in Figure 2B. Xenografts specimens ending with AI (n=3) were androgen-independent derivative of the original xenograft following androgen ablation in the host animal. All xenografts originated from HRPC patients except LuCaP 58 and LuCaP 115, which were from hormone naïve lymph node metastasis. Detailed clinical data for this set of xenografts can be found in a previous publication (ref.18).

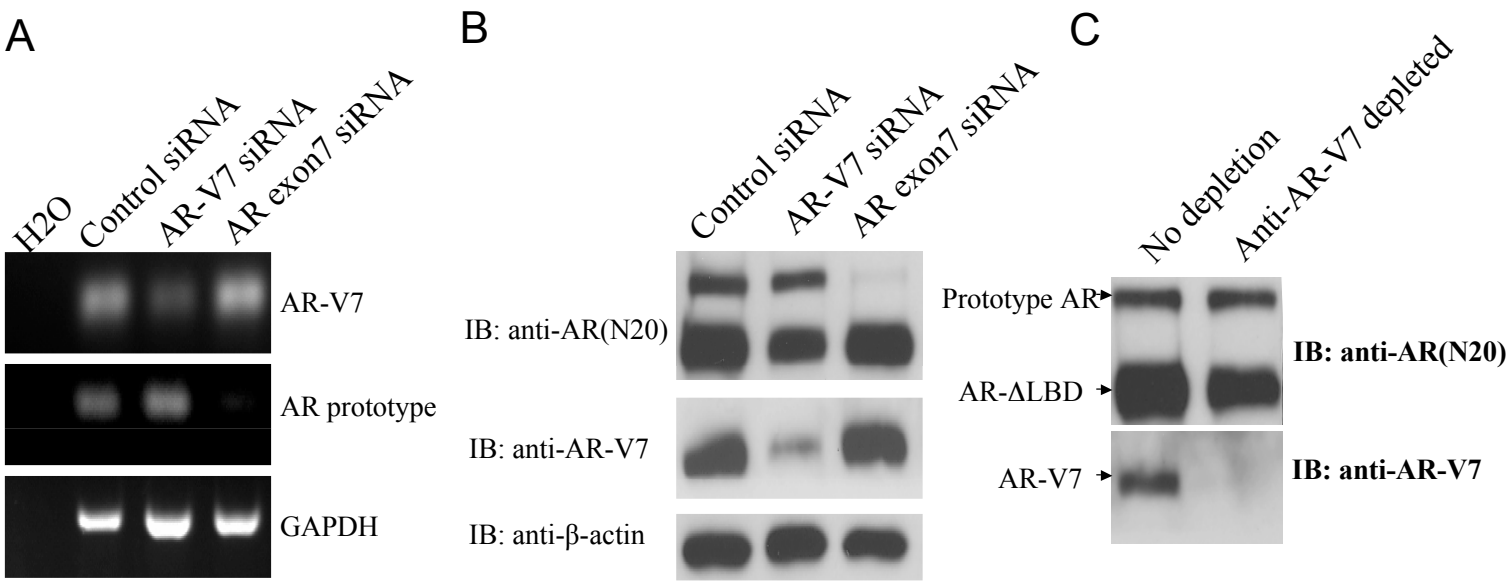

Supplemental Figure 6. Reduction of the 80KD protein band following knock down of the AR-V7 transcript or depletion of the AR-V7 protein using anti-AR-V7 antibody. A. Transcript specific knock down of prototype AR (target sequence: UCAAGGAACUCGAUCGUAU) and AR-V7 (targe sequence: GUAGUUGUGAGUAUCAUGA). B. Standard immunoblot analysis with anti-AR(N20), anti-AR-V7 and anti-β-actin antibodies following gene knock down. C. Standard immunoblot (IB) analysis with anti-AR(N20), anti-AR-V7 in CWR22Rv1 whole cell lysate following depletion of AR-V7 using anti-AR-V7 antibody . CWR22Rv1 cell lysate was incubated with protein G resin coupled to anti-AR-V7 antibody to deplete AR-V7 (anti-AR-V7 depleted) or protein G resin alone as a control (no depletion).

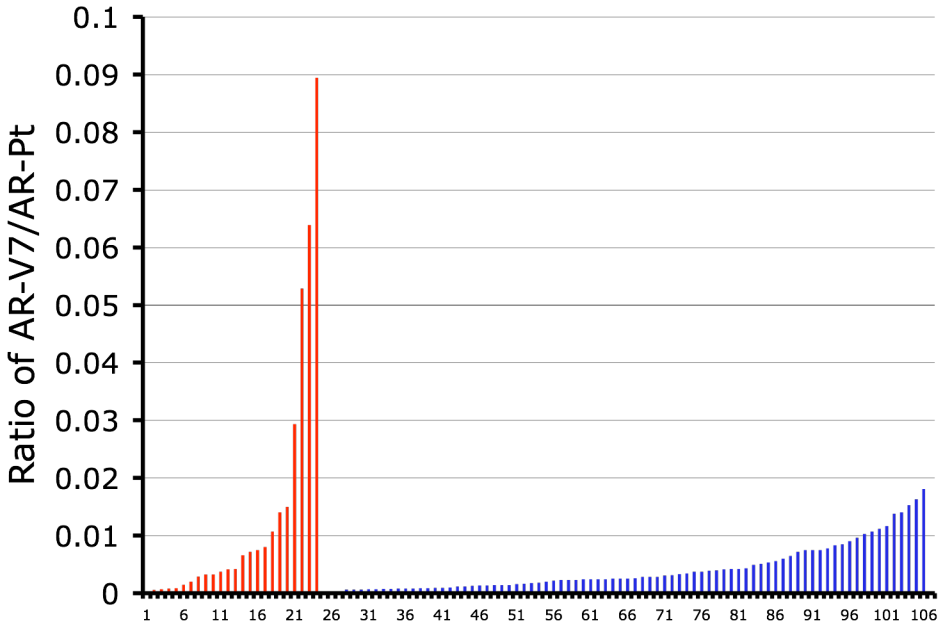

Supplemental Figure 7: Ratio of AR-V7 versus prototype AR (AR-pt) in 24 HRPC specimens (red) and 81 hormone naïve RRP cases (Blue). The cases were identical to those presented in Figure 2B, expect that 2 cases were excluded due to uncalculable ratios. Despite a trend of higher AR-V7 versus prototype AR (AR-Pt) in a subset of HRPC specimens, the overall difference between RRP (median ratio 1:389) and HRPC (median ratio 1: 238) specimens is not significant (p=0.0841, Mann-Whitney test). The absolute ratio values were calculated based on real-time RT-PCR expression values extrapolated upon standard curves of serial dilutions spanning 9 orders of magnitudes of known quantities of the target amplicons (plasmids harboring either AR-V7 or prototype AR).